RSC Advances

ROYAL SOCIETY OF CHEMISTRY

www.rsc.org/advances

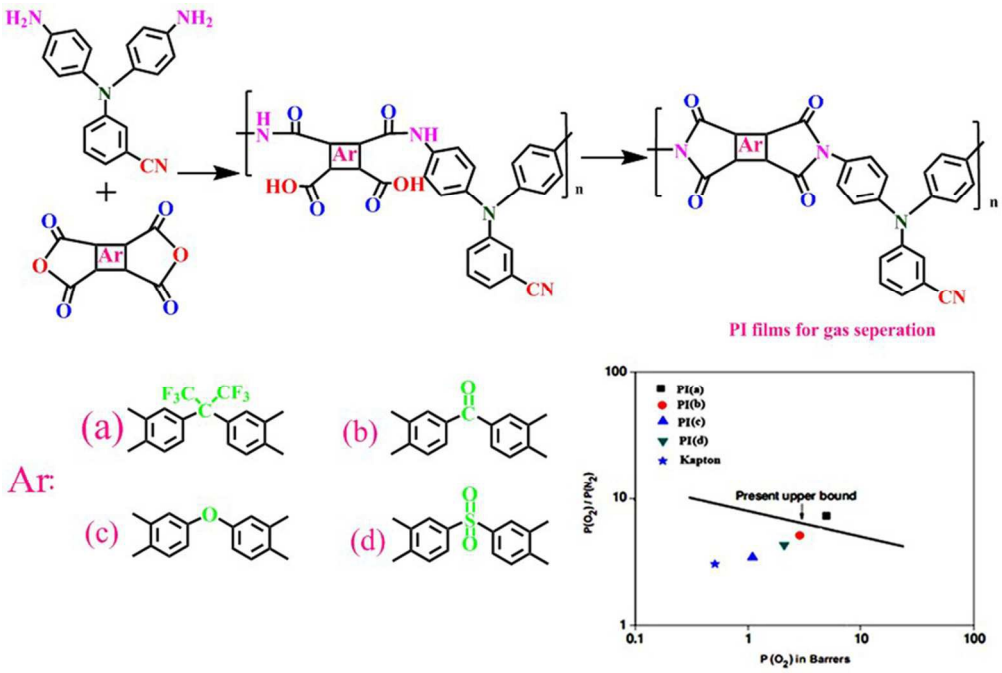

Graphical For Manuscript
46x31mm (600 x 600 DPI)

Novel highly transparent and processable polyimides with *N*-benzonitrile side chain: Thermal, mechanical and gas separation properties

Mohammad Dinari*, Hashem Ahmadizadegan

Department of Chemistry, Isfahan University of Technology, Isfahan 84156-83111, Iran

Abstract

* - Corresponding author. Tel.: +98 3133913270; fax: +98 3133912351.

E-mail address: dinari@cc.iut.ac.ir; mdinary@gmail.com

A series of organo-soluble and thermally stable polyimides (PIs) with *N*-benzonitrile side group were synthesized from a new diamine monomer, 3-(bis(4-aminophenyl)amino)benzonitrile with four different aromatic dianhydrides via thermal or chemical imidization method. The chemical structure and purity of the synthesized compounds were performed by different techniques. The inherent viscosities of the resulting PIs were in the range of 0.97-1.13 dL/g at a concentration of 0.5 g/dL in DMAc at 30 ^{o}C and these polymers were easily dissolved in organic solvents such as *N*-methyl-2-pyrrolidone, *N,N*-dimethylacetamide, and *N,N*-dimethylformamide, and tetrahydrofuran at room temperature. The obtained PIs showed reasonably high glass-transition temperature (T_g up to 291 ^{o}C) and high thermal stability (T_{10} up to 420 ^{o}C). Flexible and transparent films were obtained easily by solution casting. The membranes of these polymers showed tensile strength up to 115 MPa with elongation at break up to 13%, low water absorption (0.32-0.88%), low dielectric constant (1.98-2.38 at 1 MHz) and high optical transparency ($\lambda_{cut\text{-}off}$ up to 352 nm). The combination of excellent solubility, film quality, and thermal stability makes these PIs as potential candidates for high-performance gas separation membrane applications by solution-casting processes. Permeability measurements were made for O_2, H_2, CO_2 and CH_4 at 35 °C.

Keywords: Diamine with benzonitrile linkages; Polyimides; High performance polymers; Gas separation; Thermal stability

1. Introduction

Aromatic polyimides (PI)s are a class of thermally stable polymers due to their astonishing thermal and chemical resistance, good film forming ability, low dielectric constant, superior mechanical and physical properties as well as also excellent electrical properties.[1–4] PIs are also possessing outstanding dimensional stability under loads, which allows their use in high-temperature environments. Certainly, the presence of imide rings and subsequently charge transfer complexes in the polymer backbone lead directly to such a favorable balance of chemical and mechanical properties.[5–8] Because of the ability to maintain their properties in such a wide temperature range, PIs are applied in many industrial applications including aerospace industry as constitutional materials and structural parts, insulation materials, hot zone resins, adhesives; in electronic and microelectronic industry as dielectric materials, liquid crystal displays, memory devices, printed circuit boards, cable jackets, and wire coatings.[9-13] The functional nitrile groups may lead to the increase of thermooxidative resistance and of dielectric constant relative to the polymers that do not have this substituent on to the macromolecular chain. Also, the nitrile substituent may increase other physical properties of high performance materials, since it was shown that some amorphous polymers containing strong dipoles displayed piezoelectric response.[14-17] PIs are also commonly used as gas separation and fuel cell membranes, automotive components, medical tubing, humidity sensors, as well as fiber optic coatings.[17]

PI based gas separation membranes are anticipated to contribute in numbers of major environmental and energy technologies including gas purification and capture.[18] The requirement of high permeability and good selectivity is then considered as a main factor for the design and preparation of high performance gas separation membranes.[19] There is an inherent trade-off of gas pairs between permeability and selectivity for entirely the gas separation polymer

membranes, which was quantified in 1991 and 2008 by Robeson.[20,21] The upper bound was identified on plots of double logarithmic plots of selectivity against permeability for a wide range of gas pairs using a comprehensive list of existing polymer permeability.[20,21]

To obtain high performance PIs materials by structural modification, a high-purity 3-[bis(4-aminophenyl)amino]benzonitrile, was synthesized through a modificatory method and subsequently polycondensed with various commercially available aromatic dianhydrides including as 4,4'-(hexafluoroisopropylidene) diphthalic anhydride (6FDA or a), 4,4′-benzophenone tetracarboxylicdianhydride (BTDA or b), 4,4'-oxydiphthalic dianhydride (ODPA or c) and 3,3',4,4′-diphenylsulfone tetracarboxylic dianhydride (DSDA or d) to produce a series of PIs containing benzonitrile units (6a–e). It is hoped that these benzonitrile-containing PIs will have enhanced processability and enhanced thermal stability. The characterizations of the diamine and related intermediates, as well as the resulting polymers based on the diamine were carried out by means of elemental analyses, Fourier transform infrared (FT-IR), proton nuclear magnetic resonance (^{1}HNMR) spectroscopy, X-ray diffraction (XRD), thermogravimetric analysis (TGA), mechanical testing and differential scanning calorimetry (DSC) techniques. Also the dielectric properties, optical transparency and gas separation properties of these novel materials were studied.

2. Experimental

2.1. Materials

All materials and solvents were purchased from Merck Chemical Co and Aldrich Chemical CO. 3-Aminobenzonitrile and 1-fluoro-4-nitrobenzene, palladium on activated carbon (10 wt%), hydrazine hydrates were used as received. All the dianhydrides were recrystallized from acetic anhydride and heated at 150 ^{o}C overnight prior to use. *N*-methyl-2-pyrrolidone (NMP), *N,N*-

dimethylformamide (DMF) and *N,N′*-dimethylacetamide (DMAc) were dried over barium oxide, followed by fractional distillation.

2.2. Synthesis of diamine monomer

In a 50 mL three-neck round-bottom flask was placed 3-aminobenzonitrile (1 g, 8.46 mmol), 1-fluoro-4-nitrobenzene (2.41 g, 17.10 mmol), cesium fluoride (2.56 g, 19 mmol), and 20 mL of DMSO. The mixture was heated with stirring at 110 °C for 5 h under nitrogen. The reaction mixture was cooled and then poured in to 250 mL of ethanol. The yellow precipitate was collected by filtration and dried under vacuum. The product was purified by recrystallization from glacial acetic acid to afford 3-(bis(4-nitrophenyl)amino)benzonitrile in 90% yield; mp 218-220 °C. Hydrazine monohydrate (5 mL) was added dropwise to a mixture of dinitro compound (1.0 g, 2.77 mmol) and a catalytic amount of 10% palladium on activated carbon (Pd/C, 0.02 g) in ethanol (30 mL) at the boiling temperature. The mixture became homogeneous after 1.5 h, and the reaction was refluxed for 30h. The mixture was then filtered to remove Pd/C. After cooling, the precipitated blue crystals were isolated by recrystallization from ethanol. The yield was 81%; mp 188- 191 °C.

FTIR (KBr, cm^{-1}) of diamine: 3448 (s), 3377 (s), 3113 (w), 3075 (w), 2225(s), 1555 (m), 1535 (m) 1440 (w), 1323 (w), 1252 (w), 844 (m), 739 (w).

^{1}H-NMR (500 MHz, DMSO-d_6, ppm) of diamine: 4.49 (s, 4H, NH), 6.26-6.28 (d, 8H, Ar-H, *J*= 4.5 Hz), 6.49 (s, 1H, Ar-H), 6.76-6.78 (d, 1H, Ar-H), 7.19-7.20 (d, 1H, Ar-H, *J*= 4 Hz), 7.36-7.38 (dd, 1H, Ar-H, *J*= 4 Hz).

^{13}C-NMR (125 MHz, DMSO-d_6), of diamine, δ (ppm): 108.22 (Ar), 112.31 (CN), 118.82 (Ar), 121.18 (Ar), 123.32 (Ar), 124.12 (Ar), 125.17 (Ar), 137.25 (Ar), 138.45 (Ar), 141.35 (Ar), 148.33 (Ar).

Elemental analysis calculated for $C_{19}H_{16}N_4$ (300.36g mol^{-1}): Calcd. (%) C, 75.98%; N, 18.65 %; H, 5.37 %. Found (%) C, 75.86%; N, 18.79%; H, 5.39 %.

2.3. Synthesis of high performance PIs

Novel PIs (a-b) were synthesized by the reactions of diamine with different dianhydrides (a-b). The synthesis of PIa is employed as an example to show the general synthetic method employed to prepare the PIs. A mixture consisting of 1.00 g (3.32 mmol) of diamine, 1.47 g (3.32 mmol) of 6FDA, and 100 mL of NMP were added to a 250 mL three-necked flask which was equipped with a mechanical stirrer, a condenser and a nitrogen inlet. The reaction mixture became very viscous after 2 h. The mixture was constantly stirred for 2 h at room temperature to give poly (amic acid) (PAA). In the next step, 16.8 mL of triethylamine in 50 mL of NMP was added slowly to the reaction mixture, which was stirred for another 4 h at room temperature. The inherent viscosity of the PAAa was 1.15 dL/g, as measured in DMAc at a concentration of 0.5 g/dL at 30 °C. The PAA was converted into PI with either a thermal or chemical imidization method. In the thermal imidization method, about 2 g of the PAA solution was spread into a Petri culture dish 7 cm in diameter and baked at 90 °C overnight (ca. 12 h) for the removal of the casting solvent. The semidried PAA film was further dried and converted into the PI by sequential heating at 150 °C for 30 min, at 200 °C for 30 min, and at 250 °C for 1 h. For the elemental analysis, tensile testing, X-ray crystallography, and thermal analysis, the PI films were further heated at 350 °C for another 1 h to ensure the complete imidization. In the chemical imidization method, 5 mL of acetic anhydride and 2 mL of pyridine were added to the remaining PAA solution, and the mixture was heated at 100 °C for 1 h to affect a complete imidization. The resultant solution of the polymer was poured slowly into 250 mL of methanol, and the precipitate

was washed thoroughly with methanol and hot water, collected by filtration, and dried in air at 150 °C for 4 h.

PIa: Anal. Calcd. for $C_{38}H_{18}F_6N_4O_4$ (708.56 g/mol): C, 64.42%; H, 2.56%; N, 7.91%; Found: C, 64.48%; H, 2.53%; N, 7.85%. FT-IR (KBr, cm^{-1}): 3086 (aromatic C-H stretching), 2,225 (stretching C≡N), 1775 (asymmetric imide C=O stretching), 1722 (symmetric imide C=O stretching), 1625 (aromatic C=C stretching), 1236, 1126 (C-F stretching), and 821 (C-N bending).

^{1}H-NMR (500 MHz, DMSO-d_6, ppm): 6.26-6.27 (d, 2H, Ar-H, *J*= 3.5), 6.48-6.49 (s, 2H, Ar-H, *J*= 4.5 Hz), 6.68-7.69 (d, 2H, Ar-H, *J*= 4.5 Hz), 6.88 (s, 1H, Ar-H), 7.27-7.28 (d, 1H, Ar-H, *J*= 3.5), 7.36-7.37 (d, 1H, Ar-H, *J*= 3.5), 7.17-7.18 (d, 1H, Ar-H, *J*= 4.5 Hz), 7.66-7.68 (d, 1H, Ar-H, *J*= 3.5), 7.88-7.89 (d, 1H, Ar-H, *J*= 4.5 Hz), 8.17-8.18 (d, 1H, Ar-H, *J*= 4.5 Hz), 8.38-8.39 (d, 1H, Ar-H, *J*= 4.5 Hz).

PIb: Anal. Calcd. for $C_{36}H_{18}N_4O_5$ (586.55 g/mol): C, 73.72%; H, 3.09%; N, 9.55%. Found: C, 73.77%; H, 3.13%; N, 9.48%. FTIR (KBr, cm^{-1}): 3106 (aromatic C-H stretching), 2217 (stretching C≡N), 1777 (asymmetric imide C=O stretching), 1726 (symmetric imide C=O stretching), 1629 (aromatic C=C stretching), 825 (C-N bending).

^{1}H-NMR (500 MHz, DMSO-d_6, ppm): 6.15-6.16 (d, 2H, Ar-H, *J*= 3.5), 6.55-6.57 (s, 2H, Ar-H, *J*= 4.5 Hz), 6.62-7.64 (d, 2H, Ar-H, *J*= 4.5 Hz), 6.71 (s, 1H, Ar-H), 7.45-7.46 (d, 1H, Ar-H, *J*= 3.5), 7.53-7.55 (d, 1H, Ar-H, *J*= 3.5), 7.78-7.80 (d, 1H, Ar-H, *J*= 4.5 Hz), 7.82-7.83 (d, 1H, Ar-H, *J*= 3.5), 8.17-8.19 (d, 1H, Ar-H, *J*= 4.5 Hz), 8.26-8.28 (d, 1H, Ar-H, *J*= 4.5 Hz), 8.46-8.48 (d, 1H, Ar-H, *J*= 4.5 Hz).

PIc: Anal. Calcd. for $C_{35}H_{18}N_4O_5$ (574.54 g/mol): C, 73.17%; H, 3.16%; N, 9.75%. Found: C, 73.20%; H, 3.18%; N, 9.68%. FT-IR (KBr, cm^{-1}): 3080 (aromatic C-H stretching),

2,225 (stretching C≡N), 1777 (asymmetric imide C=O stretching), 1723 (symmetric imide C=O stretching), 1619 (aromatic C=C stretching), 826 (C-N bending).

PId: Anal. Calcd. for $C_{35}H_{18}N_4O_6S$ (622.60 g/mol): C, 67.52%; H, 2.91%; N, 9.00%, S, 5.15%. Found: C, 67.58%; H, 3.03%; N, 8.98%, S, 5.13%. FT-IR (KBr, cm^{-1}): 3116 (aromatic C-H stretching), 2,230 (stretching C≡N), 1773 (asymmetric imide C=O stretching), 1722 (symmetric imide C=O stretching), 1643 (aromatic C=C stretching), 832 (C-N bending).

2.4. Preparation of the PI films

A solution of the polymer was made by dissolving about 0.4 g of the PI sample in 2 mL of NMP. The homogeneous solution was casted onto a glass substrate and heated in oven at 80 ^oC for 8 h to remove most of the solvent; then the semi-dried film was further dried in vacuum at 150 ^oC for 8 h. The obtained films were around 30 μm thick and were used for further characterization.

2.5. Equipments

Carbon, hydrogen and nitrogen content of the compounds were determined by pyrolysis method by Vario EL elemental analyzer. ^{1}H-NMR spectra was recorded on a Bruker 500 and 125MHz instrument (Switzerland) using *N,N*-dimethylsulfoxide (DMSO-d_6) as solvent. The FT-IR spectra were taken at room temperature with a resolution of 4 cm^{-1} using 400 D IR spectrophotometer (Japan). Band intensities are assigned as weak (w), medium (m), strong (s), and broad (br). Inherent viscosity (η_{inh}) of the polymers in DMAc was measured at about 0.5 g/dL concentration with an Ubbelohde viscometer at 30±0.5 ^oC. Gel permeation chromatography (GPC) was performed with a Waters instrument (Waters 2414) and tetrahydrofuran (THF) was used as eluent (flow rate 0.5 mL/min). Polystyrene was used as standard and RI detector was used to record the signal in GPC. DSC measurements were made on a DSC Q200 instrument at a heating/cooling rate of 20 ^oC min^{-1} under nitrogen. The glass transition temperature (T_g) was

taken at the middle of the step transition in the second heating run. Thermal decomposition of these polymers was measured on a TA Instruments thermo gravimetric analyzer, Model TGA-2950. A heating rate of 20 ^{o}C min^{-1} was used for determination of the decomposition temperature (T_d) under air. Tensile strength and elongation at break of thin PI membranes were measured with the help of UTM-INSTRON, PLUS, Model No. 8800. Test samples with dimension of 10×25 mm^2 and thickness in the range of 0.060 to 0.070 mm were used for the measurement of tensile strength and percentage of elongation at break. The dielectric constants of the PI films were calculated from the capacitance values, measured by the parallel plate capacitor method using HIOKI 3532-50 LCR Hi Tester at 1 MHz at a temperature of 30 ^{o}C and a relative humidity of 45. Water absorption of the films were measured using a Mettler microbalance of sensitivity of 10-6 g after immersing the films in double distilled water for 72 h at 30 ^{o}C. Ultra violet spectra of the polymer films were recorded at room temperature using Detector SD–2000 (Ocean Optics Inc.) and source lamp DH–2000. The XRD patterns were collected by using a Philips Xpert MPD X-ray diffractometer. The diffractograms were measured for 2θ, in the range of 10–80º, using a voltage of 40 kV and Cu Kα incident beam (λ=1.51418 Å). The densities of the membranes were measured using Wallace High Precision Densimeter-X22B (UK) using water displacement method. The gas transport properties of the PI membranes were studied at 3.5 bar of applied gas pressure and at 35 ^{o}C using automated Diffusion Permeameter (DP-100-A) manufactured by Porous Materials Inc., USA. Ultrahigh pure (99.99 %), methane, nitrogen, oxygen, and carbon dioxide gases from BOC Gases, were used for the permeation study. The permeability coefficient, ideal permselectivity (α), diffusion coefficient (D), ideal diffusivity selectivity (α_D), solubility coefficient (S), and ideal solubility selectivity (α_S) were determined

according to reported procedure.[22] The reproducibility of the measurements was checked from three independent measurements using the same membrane and it was better than ±5%.

2.6. Measurements of gas transport properties

The permeation cell was placed in a thermostatically controlled housing for maintaining isothermal measurement conditions. The effective permeation area (A) was 5.069 cm^2. The membranes were degassed for at least 10 h at 35 ^oC within the permeation cell prior to the gas permeation study. To the upstream side of the membranes, the gas pressure (p_i = 3.5 bar) was applied instantaneously and in the downstream side a reservoir of constant volume (119 cm^3) was connected with a pressure transducer to observe the total amount of gas which passed through the membranes. The time-lag method was used for the gas transport measurements. This technique allows the determination of mean permeability coefficient (P) from the steady state gas pressure increment $(dp/dt)_s$ in the calibrated volume V of the product standard temperature and pressure (T_0 = 273.15 K, p_0 = 1.026 bar), T is the temperature of measurement, d is the thickness of the membrane and $(dp/dt)_s$ was obtained from the slope of the increments of downstream pressure vs. time plot. The reproducibility of the measurements was better than ±5% for CO_2 and O_2 permeability measurement but the reproducibility was in the range of ±10% for CH_4 and N_2 permeability measurements. The mean permeability coefficient was determined from Eq. (1):

$$p = \left[\frac{VdT_0}{Ap_i p_0 T}\right]\left(\frac{dp}{dt}\right)_s \qquad (1)$$

Permeability coefficient (P) is a product of diffusivity (D) and solubility coefficient (S). The solubility coefficient S was calculated from Eq. (2):

$$S = \frac{P}{D} \qquad (2)$$

Diffusion coefficient (D) was calculated from the time-lagθ according to Eq. (3):

$$D = \frac{d^2}{6\theta} \qquad (3)$$

The ideal permselectivity of the polymer membranes for a pair of gases A and B is the ratio of the individual permeability and can be expressed according to the follows Eq. (4):

$$\alpha_{P(A/B)} = \frac{P_A}{P_B} \qquad (4)$$

3. Results and discussion

3.1. Preparation and characterization of the diamine monomer

A specific diamine was prepared via a two-step procedure: firstly, nucleophilic substitution reaction of 3-aminobenzonitrile with 1-fluoro-4-nitrobenzene resulted in preparation of 3-(bis(4-nitrophenyl)amino)benzonitrile. Reduction of nitro group in the second step by hydrazine in the presence of Pd/C led to preparation of the diamine compound with benzonitrile pendent group (Scheme 1).

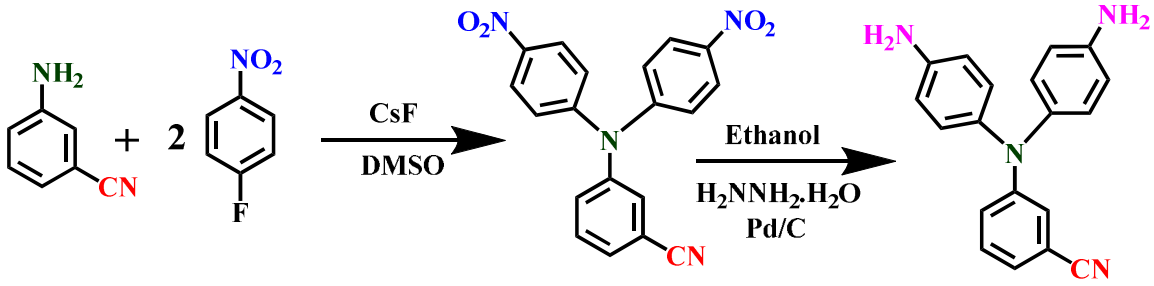

Scheme 1. Synthesis of diamine with benzonitrile pendent group.

The chemical structure of the synthesized diamine was clearly confirmed by FT-IR, ^{1}H-NMR and ^{13}C-NMR spectroscopy and elemental analysis techniques. Good agreement between calculated and found amounts of C, H, and N content was observed in elemental analysis of diamine approving its proposed structure. The FT–IR absorptions related to the nitrile group is

appeared at 2225 cm^{-1}. The familiar double absorption peaks of amine functions N–H are obvious around 3448–3377 cm^{-1}. In ^{1}H-NMR spectrum of the diamine compound (Fig. 1), a peak at 4.50 ppm was assigned to the amine protons group and all aromatic protons appeared at 6.25-7.38 ppm. Further confirmation about the structure of diamine was derived from the ^{13}C-NMR spectrum (Fig. 2), where the peak for carbon atom of nitrile group was observed at 112.31 ppm. Also, the peaks for carbon atoms of aromatic rings were observed in the range of 108.22-148.33 ppm. Thus, the NMR data and elemental analysis confirmed that the structure of the diamine agreed with the proposed molecular structure.

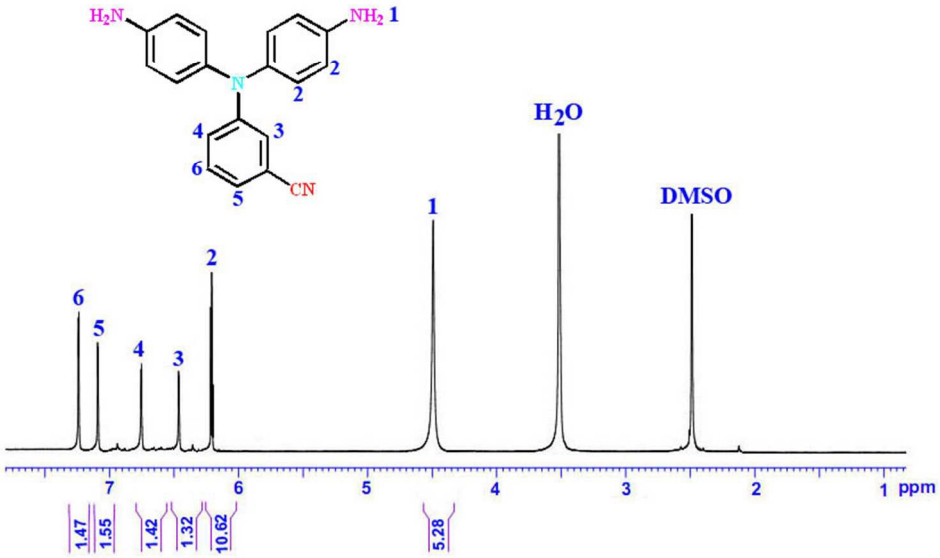

Fig. 1. ^{1}H-NMR (500 MHz) spectra of diamine in DMSO-d_6 at R.T.

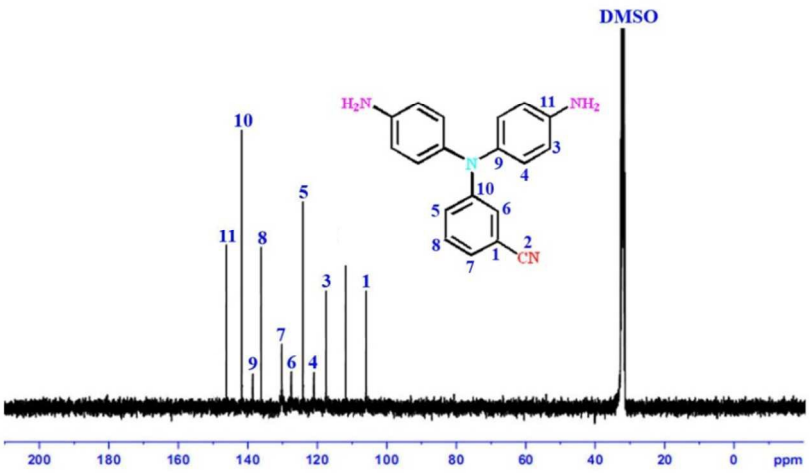

Fig. 2. ^{13}C-NMR (125 MHz) spectra of diamine in DMSO-d_6 at R.T.

3.2. Preparation and characterization of the polymers

Solution polycondensation reactions of the synthesized diamine with different aromatic dianhydrides (6FDA, BTDA, OPDA and PSDA) were performed for preparation of four novel PIs as shown in Scheme 2. The polycondensation reaction was carried out via a two-step procedure: firstly, the diamine was reacted with dianhydride at room temperature to produce PAA. In the second step, resulted PAA was cyclo-imidized and converted to relate PIs. As shown in Table 1, the obtained polymer showed inherent viscosities between 0.97 and 1.13 dL/g at a concentration of 0.5 g dL^{-1}. This was further supported by gel permeation chromatography (GPC) measurements which gave Mn, Mw and polydispersities (Mw/Mn) in the range 72380-77894, 141000-152000 and 1.90-2.10, respectively.

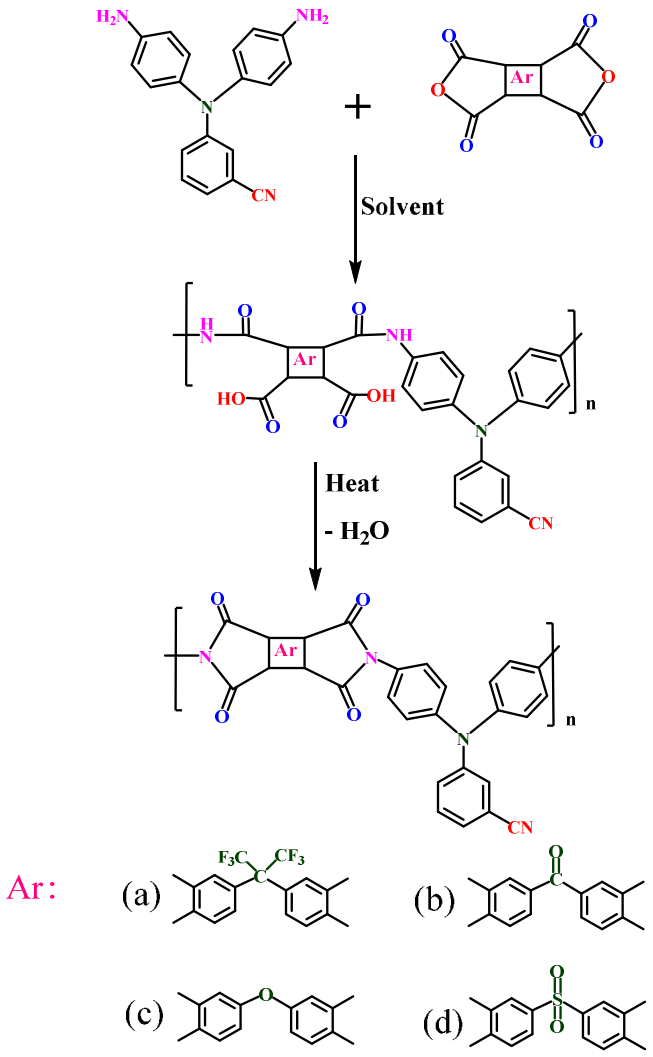

Scheme 2. Synthesis of organo-soluble PIs.

Table 1. Molecular weight characterization of the PIs.

Sample	η_{inh}(dL/g)[a]	Mn[b]	Mw[c]	PDI[d]
PIa	1.13	72380	152000	2.1
PIb	0.97	74210	141000	1.9
PIc	1.05	77894	148000	1.9
PId	1.02	-	-	-

[a]Inherent viscosity of the PAAs precursor measured at a concentration of 0.5 g/dL in DMAc at 30 °C. [b]Mn: Number average molar mass. [c]Mw: Mass average molar mass. [d]Polydispersity index: Mw/Mn.

3.3. Spectroscopic analysis

Conversion of the PAAs to the fully cyclized PIs was proved by means of by FT-IR, ^{1}H NMR spectroscopy and elemental analysis. All PAAs showed a broad absorption characteristic band of carboxylic O–H and amide N–H groups at about 2600-3700 cm^{-1} and a narrow characteristic band at 1685 cm^{-1} associated to C=O of amide linkage. Also the nitrile group is appeared at 2227 cm^{-1}. Complete imidization reaction of PAAs and formation of PIs were confirmed by FT-IR spectroscopy. The FT-IR spectra of the PIs showed the characteristic absorption bands of the imide absorption at 1777 (C=O asymmetric stretching), 1722 (C=O symmetric stretching), 1353 (C–N stretching), and 702 cm^{-1} (C=O bending). The disappearance of absorption in the region 2600–3700 cm^{-1} (O–H and N–H stretch) and around 1685 cm^{-1} (amide C=O stretch) confirms that PAAs completely conversed into PIs. The FT-IR spectra of the PAA and corresponding PI based on 6FDA and PI based on BTDA are presented in Fig. 3.

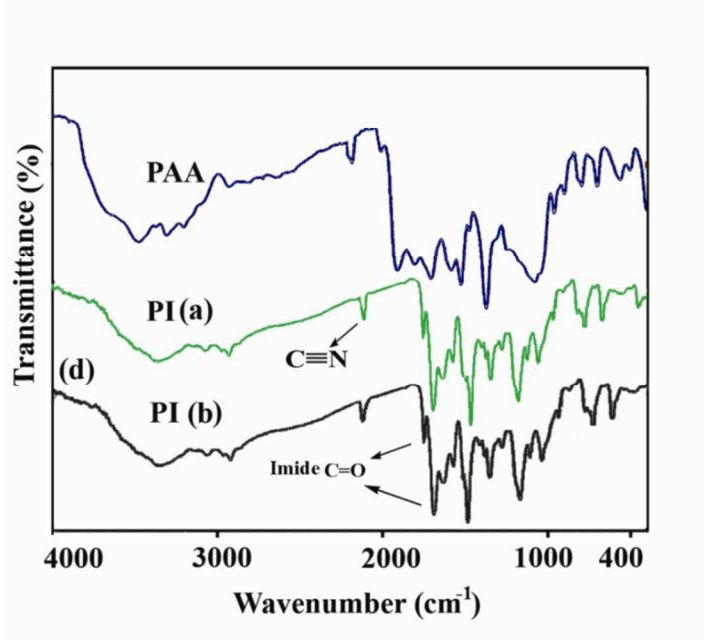

Fig. 3. FT-IR spectrum of the PAA, PIa and PIb.

Figs. 4 exhibit a typical ^{1}H-NMR spectra of the PI based on 6FDA (a), in which all the peaks have been readily assigned to the hydrogen atoms of the repeating unit and no amide or

acid protons at 10-12 ppm appears, indicating that complete imidization was really achieved and PAA film converted into PI. The assignments of each proton designated in the ^{1}H-NMR spectrum are in complete agreement with the proposed polymer structures. The sharp peaks at 4.50 ppm corresponding to the amine protons in ^{1}H-NMR spectrum of diamine disappear completely here, and new peaks appear at 7.50-8.40 ppm which correspond to the protons in the dianhydride units (Fig. 4). All PIs were also recognized by elemental analysis, which were in good agreement with the calculated ones of the proposed structures. These results show that the synthesis of new PIs should be successful and practical in this work.

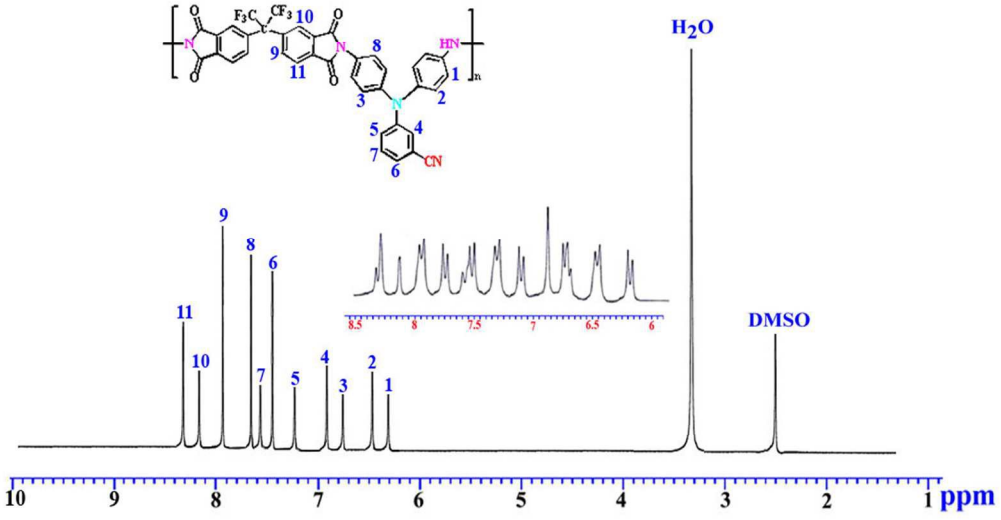

Fig. 4. ^{1}H-NMR (500 MHz) spectra of PIa in DMSO-d_6 at R.T.

3.4. Solubility

It is well known that aromatic PIs generally show rather poor solubility in organic solvents in full imidation formation, especially for some PIs derived from rigid dianhydrides such as PMDA. To enhance the solubility, bulky groups, flexible linkages or noncoplanar structures have been introduced along the polymer chains.[23-25] It should be noted that good solubility in low-boiling-point solvents is critical for preparing films or coatings at a relatively

low processing temperature, which is desirable for advanced microelectronics manufacturing applications. The solubility of the obtaining polymers was examined by dissolving 10 mg of the PIs in 1 mL several organic solvents at ambient temperature or upon heating, as shown in Table 2. It can be seen that all the PIs, can be dissolved in polar solvents, such as NMP, DMF, DMAc, and DMSO, at ambient temperature. The solubility varied depending on the dianhydrides used. PIa based on 6FDA, possessed good solubility owing to the excellent flexibility of hexafluoroisopropylidene structure in 6FDA and could be dissolved readily in DMSO, NMP, DMF, DMAc, m-cresol and THF, at ambient temperature. Also for PIc, the presences of flexible ether chain in the dianhydride unit reduce the rigidity of polymer chain and the solubility was increased. Other PIs also have fairly good solubility. The good solubility of these PIs might be attributed to the presence of the polar nitrile linkage and the polarizability resulting from the nitrogen atom in the side chain.

Table 2. Inherent viscosity (η_{inh}), film properties, and solubility behavior of the PIs (a-d).

Polymer	Solubility[a]					
	NMP	DMAc	DMF	DMSO	m-cresol	THF
PIa	++	++	++	++	±h	±
PIb	++	++	++	++	-	±
PIc	++	++	++	++	++	±
PId	++	++	++	++	-	±

[a]Qualitative solubility was tested with 10 mg of a sample (chemically imidized) in 1 mL of the solvent. += soluble at room temperature; +h = soluble on heating; -= insoluble.

3.5. X-ray diffraction

XRD was used to determine the crystalline morphology of the resulting pyridine-containing PIs, and the patterns are shown in Fig. 5. All the XRD patterns of the thermally cured PI films showed a diffuse characteristic diffraction peak at around 2θ=16-30° and no distinct crystal peaks, these should be the evidences that the PIs held completely amorphous structures. Furthermore, the amorphous character is also supported by the reasonable solubility of PIs,

which is in agreement with the general rule that the solubility decreases with increasing crystallinity.

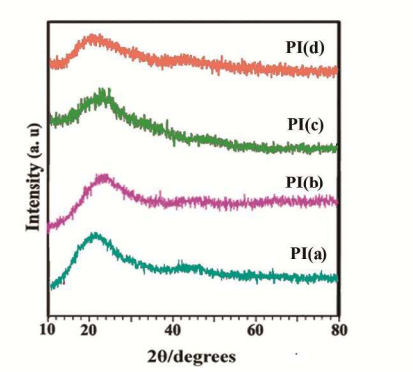

Fig. 5. XRD patterns of PIa-PId.

3.6. Mechanical properties of PI films

PI films were subjected to tensile testing and their stress-strain curves were shown in Fig. 6. Table 3 exhibits the mechanical properties of the PIs, including the tensile strength, tensile modulus, and elongations to break. These films had tensile strength of 90-115 MPa, elongations at breakage of 13-20 %, and tensile moduli of 1.29-1.68 GPa which shows strong and hard materials. PIa derived from the aromatic dianhydride 6FDA, shows small tensile strength of 95 MPa which could be attributed to the rigid structure of polymer backbone.

Table 3. Tensile and dielectric properties of the PIs.

Polymer	Modulus[a] (GPa)	Ultimate strength[b] (MPa)	Ultimate elongation[c] (%)	Water absorption at 30 °C (%)	Dielectric constant at 30 °C (1MHz)
PI(a)	1.29	95	17	0.32	1.98
PI(b)	1.43	102	15	0.56	2.23
PI(c)	1.68	115	13	0.88	2.14
PI(d)	1.34	90	20	0.43	2.38

[a] Initial slope of the stress strain curve. [b] Stress at break. [c] Elongation at break.

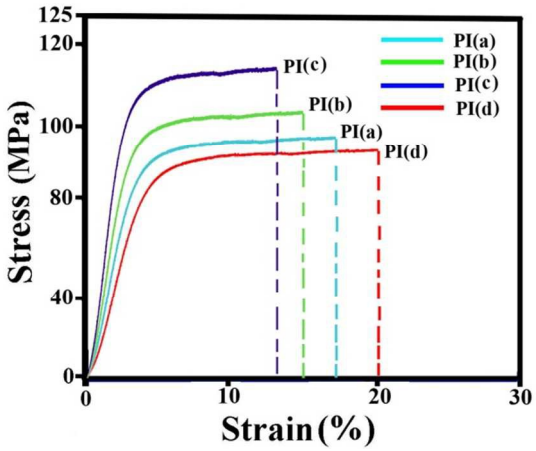

Fig. 6. Tensile stress-strain curves of the PI films.

3.7. Water absorption and dielectric properties

Water absorption is a great concern when the polymers are used in electronic packaging as dielectric insulation.[26,27] The absorbed water in the polymer structure affects their dielectric performance. Hence, for materials designed for such type of applications the water absorption data is an essential parameter. The water absorption of the PIs membranes was measured at 30 ^{o}C (Table 3). The water absorption values for these PIs were between 0.32 to 0.88%. PIa showed lowest water absorption among all the synthesized polymers due to the presence of hydrophobic -CF_3 groups in the anhydride moiety which is similar to the previous study.[28,29]

The dielectric constant of PI membrane was measured by using a capacitance meter (1 MHz at 30 ^{o}C, RH 45%). The dielectric constant and the dissipation factor are the important properties to determine the use of a material in interlayer dielectrics. The dielectric constant values of the PI membranes were presented in Table 3. In general, the PIs exhibited low dielectric constant values. This should be attributed to the incorporation of bulky benzonitrile substituents. The increasing order of dielectric constant followed the order as PId > PIb > PIc > PIa. The lower dielectric constant values may be attributed to the presence of bulky -CF_3 groups which hinders close interchain packing and to the low polarizability of the C-F bonds.[28-30]

Among the PI films, PIa showed the lowest dielectric constant (1.98) and had a decrease of 1.5 compared to that of the commercial Kapton films (3.48). This can be explained by the additional of fluorine moiety.

3.8. Thermal properties

The thermal properties of the benzonitrile -containing polymers were evaluated by TGA at the heating rate of 20 ^{o}C min^{-1} from 20 to 800 ^{o}C under N_2 flow. Fig. 7 shows the TGA curves of the synthesized PIs, and the thermal behavior parameters are listed in Table 4. The obtained PIs did not exhibit obvious weight loss before 365 ^{o}C, indicating that no thermal decomposition had occurred. As shown in Fig. 7, the decomposition-starting temperatures were in the range of 366-400 ^{o}C. The 5 and 10 % weight loss temperatures ($T_{5\%}$ and $T_{10\%}$) were in the ranges of 366-403 ^{o}C and 400-420 ^{o}C, respectively. The results showed that PIa, prepared from 6FDA, showed the best thermal stability. The amount of carbonized residue (char yield or CR) of PIs was from 66 to 72% at 800 °C under a nitrogen gas flow, depending on the structure of dianhydride component. The high char yields of these polymers can be attributed to their high aromatic content.

DSC was applied to determine glass transition temperature (T_g) of the PIs. As seen from Table 4, all the PIs exhibited T_g values higher than 291 °C, possibly because the films have high stiffness, which is mainly ascribed to the structure of the repeating units, stiffness of the polymer backbones and polymer intermolecular forces. As the diamine used for preparing the PIs was completely similar, the different T_g values resulted mainly from the different rigidities of the dianhydrides. For PIa, CF_3 groups may have led to increased chain rigidity, which consequently led to a much higher T_g.

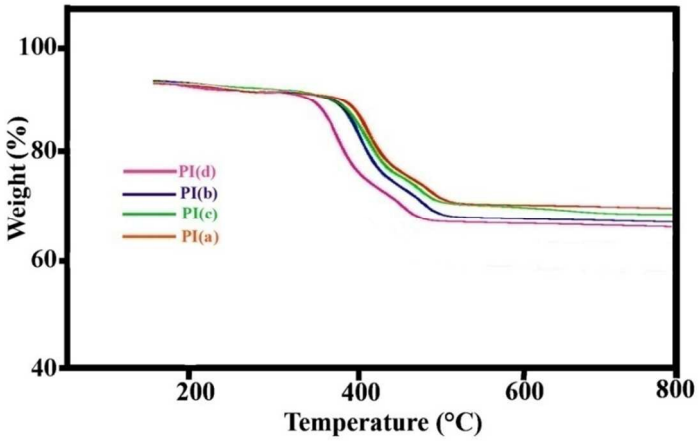

Fig. 7. TGA thermograms of PIa-PId.

Table 4 Thermal characterizations of PIs (a-b) films.

Entry	Material	T_5[a] (ºC)	T_{10}[a] (ºC)	Char yield (%)[b]	T_g[c] (°C)
1	PIa	403	420	72	299
2	PIb	402	418	70	296
3	PIc	400	412	69	295
4	PId	366	400	66	291

[a]Temperature at which 5 and 10% weight loss was recorded by TGA at a heating rate of 20 ºC/min in a nitrogen atmosphere.
[b] Percentage weight of material left undecomposed after TGA analysis at maximum temperature 800ºC in a nitrogen atmosphere
[c] Measured at a heating rate of 20 °C min^{-1} under N_2 atmosphere

3.9. Optical transparency

Thin films of PIs (a-b) were measured for optical transparency with UV–vis spectroscopy. Fig. 8 exhibits the UV-vis transmittance spectra of the PI films. The cut-off wavelength (absorption edge, λ_0) values and the percentage of transmittance at 500 nm from these spectra were listed in Table 5. The most polymers between the UV and visible area show strong absorption due to the highly conjugated aromatic structures and intermolecular charge-transfer complex formation of PI.[31] The cut-off wavelength value (352-362 nm) and the percentage of transmittance (80-83 %) at 500 nm for these PI membranes are tabulated in Table 5. The trifluoro methyl groups and flexible ether linkages in the dianhydrides moieties are very much effective in decreasing charge

transfer complex formation and improve the optical properties of the PIs.[29,31,32] The PIa showed highest optical transparency this is due to the presence of trifluoro methyl groups in anhydride part.

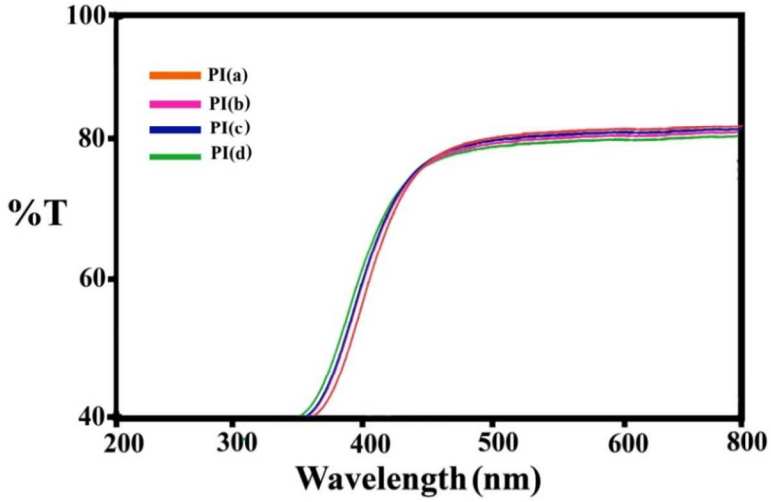

Fig. 8. UV-visible absorption spectra of PIa-PId.

Table 5. Optical transparency from UV-vis spectra of PIs

Polymer	λ_0[a] (nm)	T_{500}[b] (%)	δ (μm)[c]
PIa	362	83	33
PIb	355	81	35
PIc	355	82	34
PId	352	80	34

[a]λ_0: Cutoff wavelength of the polymer films.

[b]T_{500}: Transmittance at 500 nm.

[c]δ: The measured thickness of the film samples.

3.10. Gas separation performance test

Gas transport properties of four different gases (CO_2, O_2, N_2, CH_4) through these newly synthesized aromatic PIs were studied at 35 ^oC under an upstream pressure of 3.5 bar. It is well known that permeability coefficient varies depending on various casting protocols adopted in

different laboratories. However, the ideal permselectivity value for a pair of gas can be considered as a standard parameter to compare gas separation performance of a series of polymeric membranes with other polymeric membranes measured in other laboratories.[33] Gas permeability coefficients and permselectivity values have been presented in Table 6. The diffusion coefficients and solubility coefficient values are shown in Table 7. The solubility selectivity and diffusivity selectivity values have been also depicted in Table 7. Since we could not carry out direct sorption measurements for these four polymeric membranes due to limited equipment, definitely, a direct sorption measurement could provide a better insight on the permeation mechanism and more reliable diffusion coefficient values. The diffusion coefficients were determined using the time-lag value of gas flow vs. time plot. We understand that the diffusion coefficient values determined from time-lag values are unreliable when the dual mode transport characteristics apply but within a series of polymers the measured values of diffusion coefficients can be used for the comparative study of their general behavior.[34]

Table 6. Gas transport characteristics of PI films

Film	$P(O_2)$	$P(N_2)$	$P(CO_2)$	$P(CH_4)$	$P(O_2)/P(N_2)$	$P(CO_2)/P(CH_4)$	$P(CO_2)/P(O_2)$	$P(CO_2)/P(N_2)$	Ref.
PIa	7.05	0.84	16.77	0.22	8.40	76.22	2.38	19.96	-
PIb	2.14	0.55	7.76	0.31	3.90	25.03	3.63	14.11	-
PIc	1.12	0.34	3.76	0.21	3.29	17.90	3.36	11.06	-
PId	3.33	0.44	10.08	0.76	7.57	13.26	3.03	22.91	-
Kapton	0.64	0.11	3.51	0.06	5.82	58.50	5.48	31.91	2

Permeability coefficient (P) in barrer (1 barrer) 1 cm^3 (STP) cm cm^{-2} s^{-1} $cmHg^{-1}$ $\times 10^{-10}$), measured at 35 °C.

Table 7. Gas diffusion coefficients D×10^8 (cm^2/s) and solubility coefficients S in 10^{-2} cm^3 (STP)/cm^3 cm Hg of the PIs at 35 °C and 3.5 bar.

Polymer	CO_2		O_2		$(CO_2)/(CH_4)$		$(O_2)/(N_2)$	
	D	S	D	S	α_D[a]	α_s[a]	α_D	α_s
PIa	2.98	8.54	8.22	1.98	2.58	10.65	1.94	0.64
PIb	1.44	2.93	4.76	0.95	1.93	7.54	1.15	0.78
PIc	0.88	2.22	2.99	0.66	0.38	8.92	0.42	1.34
PId	1.88	4.96	5.86	0.94	1.08	10.12	0.92	1.55

α_D = diffusivity selectivity values of gas pairs (D_A/D_B). α_S = solubility selectivity values of gas pairs (S_A/S_B).

Fractional free volumes (FFVs) for all the PI membranes with respect to four different gases were estimated using group contribution method developed by Park and Paul.[33] The order of fractional free volume for the PI membranes for all the gases was PIa > PId > PIb >PIc (Table 8). Incorporation of hexafluro linkage in the main chain is known to render loose chain packing consequently PIa have higher fractional free volume in the series.[36] The order of gas permeability coefficients of four PI membranes for all the gases was PIa > PId > PIb > PIc. This decreasing trend of permeability coefficient of these PIs (from 'PIa' to 'PId') nicely correlates with their corresponding FFV values for all the gases.[35] The dependence of permeability coefficients with FFV of the PIs for the four gases (CO_2, O_2, N_2 and CH_4) is represented in Table 8.

For amorphous polymers the logarithm of permeability is found to decrease almost linearly with the increasing reciprocal fractional free volume.[36] All the synthesized PIs follow the above trend. For all the PIs, the gas permeability coefficient follow the order as P (CO_2) >P (O_2) > P (N_2) > P (CH_4) which is basically the reverse order of their kinetic diameter (Å): CO_2 (3.3) <

O_2 (3.46) < N_2 (3.64) < CH_4 (3.8). The order of diffusion coefficient for the PIs followed the order as D (O_2) > D (CO_2) > D (N_2) > D (CH_4). A different order of diffusion coefficients compared to the permeability coefficients order for these four gases can be explained by the fact that there is no or little interaction between O_2, CH_4, and N_2 with the PIs. However, there is some sort of interaction between CO_2 and PIs. The interaction is due to the fact that PI has imide linkage in chain repeating unit. Permeability of CO_2 through each PIs was higher than the other gases due to the higher solubility coefficient values of CO_2 for each PIs.[37] From Tables 6 and 7 it can be interpreted that ideal permselectivities for CO_2/O_2, CO_2/N_2 and CO_2/CH_4 gas pairs are mainly due to the solubility selectivities as diffusivity selectivities are reasonably small.[38]

Table 8. Fractional free volumes and observed density of the polymers.

Polymer	Density[a]	$(FFV^b)_{CH4}$	$(FFV^b)_{N2}$	$(FFV^b)_{O2}$	$(FFV^b)_{CO2}$
PIa	1.08	0.21	0.23	0.25	0.22
PIb	1.52	0.10	0.12	0.11	0.11
PIc)	1.32	0.14	0.13	0.11	0.12
PId	1.38	0.14	0.17	0.19	0.16

[a] Density (g/cm^3) measured at 30 °C.

[b]FFV = $[V-(V_o)_n]/V$, where V is the volume per mole of the repeat unit of the polymer at 30 °C, $(V_o)_n = \sum\gamma_{nk}(V_w)_k$, γ_{nk} is set of empirical factors depending upon gas 'n' and group 'k'. $(V_w)_k$ represents van der Waals volumes for group 'k'.[35]

The ideal gas separation performances of this polymeric membrane have been compared with commercially available polymer membrane (Kapton). For a better comparison, the gas separation performances of these PIs in comparison to the other polymers have been presented as Robeson plots [20,21] of permselectivity of O_2/N_2 gas pair vs. permeability of O_2 (Fig. 9) and

permselectivity of CO_2/CH_4 gas pair vs. permeability of CO_2 (Fig. 10). In comparison to Kapton, these polymers showed excellent permeability with better separation performances for both O_2/N_2 and CO_2/CH_4 gas pairs. Especially, PIa showed higher permeability as well as higher permselectivity for CO_2/CH_4 and O_2/N_2 gas pairs in comparison to the kapton and PIb surpassed the upper boundary limit drawn by Robeson for O_2/N_2 gas pair.[20,21]

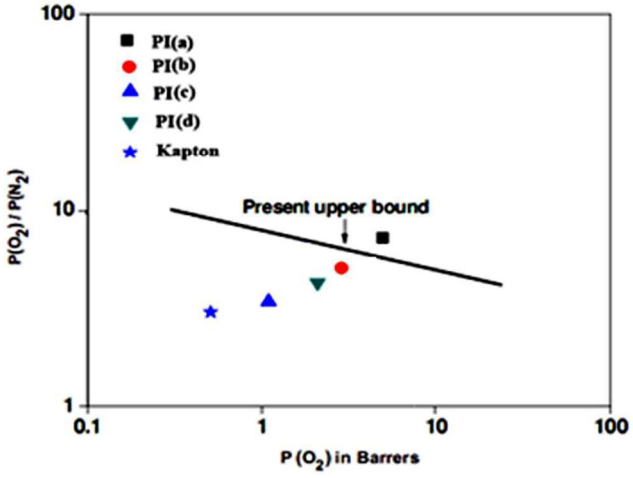

Fig. 9. Robeson plots of selectivity versus permeability for the PIa-PId membrane.

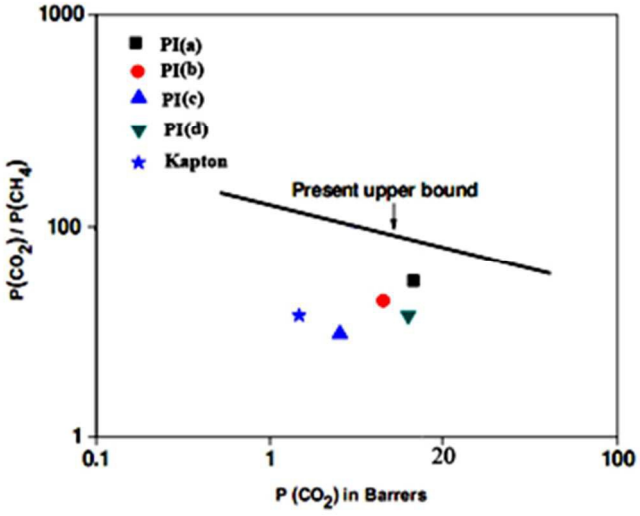

Fig. 10. Robeson plots of selectivity versus permeability for the PIa-PId membrane.

4. Conclusion

A series of processable PIs with benzonitrile pendant group were synthesized from a diamine monomer, 3-(bis(4-aminophenyl)amino)benzonitrile with four different aromatic dianhydrides via thermal or chemical imidization method. The resulting polymers showed good solubility in polar amidic solvents, excellent thermal stability, and high glass transition temperatures. The solutions of intermediate PAA could be cast into flexible films with good mechanical properties and optical transparency, and low dielectric constants. Transparent and flexible membranes with very good thermal and mechanical properties made PIs suitable candidates for membrane based gas permeation study. Gas transport properties of CO_2, O_2, N_2, and CH_4 through these newly synthesized PI membranes were successfully. All the PIs showed almost similar permeability coefficients with different permselectivity values except PIb. PIa exhibited very high permeability for all the gases with higher permselectivity for different gas pairs and surpassed the upper boundary limit drawn by Robeson for O_2/N_2 gas pair. Dielectric properties for these PIs were determined and used to correlate with their permeability coefficients. The incorporation of benzonitrile units into the polymer backbone leads to soluble polymeric materials that are amenable for use as high-performance materials and demonstrate a promising potential for future application.

Notes

The authors declare no competing financial interest.

Acknowledgements

We wish to express our gratitude to the Research Affairs Division Isfahan University of Technology (IUT), Isfahan, for partial financial support. Further financial support from National Elite Foundation (NEF), and Iran Nanotechnology Initiative Council (INIC) is gratefully acknowledged.

References

(1) Ghosh, M. K.; Mittal, K. L. *Polyimides: Fundamentals and Applications*. Marcel Dekker, New York, **1996**.

(2) Zhang, Q. H.; Luo, W. Q.; Gao, L. X.; Chen, D. J.; Ding, M. X. Thermal Mechanical and Dynamic Mechanical Property Of Biphenyl Polyimide Fibers. *J. Appl. Polym. Sci*. **2004**, *92*, 1653–1657.

(3) Zhang S. J.; Li Y. F.; Yin D. X.; Wang X. L.; Zhao X.; Shao Y.; Yang S. Y. Study on Synthesis and Characterization of Novel Polyimides Derived from 2,6-Bis(3-aminobenzoyl)pyridine. *Eur. Polym. J*. **2005**, *41*, 1097–1107.

(4) Mallakpour, S.; Dinari, M. In Situ Fabrication of Highperformance Polyimide/Tyrosine-Modified Layered Silicate Nanocomposites. *Nano*. **2012**, *7,* 1250021, p1-p10.

(5) Hergenrother, P. M.; Watson, K. A.; Smith, J. G.; Connell, J. W.; Yokota, R. Polyimides from 2,3,3′ ,4′-Biphenyltetracarboxylic Dianhydride and Aromatic Diamines. *Polymer* **2002**, *43*, 5077–5093.

(6) Verker R.; Atar N.; Quero F.; Eichhorn SJ.; Grossman E. Tensile Stress Effect on the Macromolecular Orientation and Erosion Mechanism of an Atomic Oxygen Irradiated Polyimide. *Polym. Degrad. Stab*. **2013**, *98*, 997–1005.

(7) Kong, J. Y.; Choi, M. C.; Kim, G. Y.; Park, J. J.; Selvaraj, M.; Han, M. J.; Ha, C. S. Preparation and Properties Of Polyimide/Grapheme Oxide Nanocomposite Films With Mg Ion Crosslinker. *Eur. Polym. J*. **2012**, *48*,1394–1405.

(8) Dinari, M.; Ahmadizadegan, H. Preparation, Characterization and Gas Separation Properties of Nanocomposite Materials Based on Novel Silane Functionalizing Polyimide Bearing Pendent Naphthyl Units and ZnO Nanoparticles. *RSC Adv.* **2015**, *5*, 8630-8639.

(9) Chao, D.; Wang, S.; Yang, R.; Berda, E. B.; Wang, C. Synthesis and Properties of Multifunctional Poly(Amic Acid) With Oligoaniline and Fluorene Groups. *Colloid Polym. Sci*. **2013**, *291*, 2631–2637.

(10) Saleh, M.; Lee, H. M.; Kemp, K. C.; Kim, K. S. Highly Stable CO_2/N_2 and CO_2/CH_4 Selectivity in Hyper-Cross-Linked Heterocyclic Porous Polymers. *ACS Appl. Mater. Interfaces*, **2014**, *6,* 7325–7333.

(11) Waris, G.; Siddiqi, H. M.; Bolte, M.; Hossain, R.; Akhtar, Z. Synthesis and Characterization of Processable Aromatic Polyimides and Their Initial Evaluation as Promising Biomaterials. *Colloid Polym. Sci*. **2013**, *291*, 1581-93.

(12) Madhra, MK.; Salunke, AK.; Banerjee, S.; Prabha, S. Synthesis and Properties of Fluorinated Polyimides Derived from Novel 2,6-Bis(3′-trifluoromethyl-p-aminobiphenyl ether) Pyridine and 2,5-Bis(3′-trifluoromethyl-p-aminobiphenyl ether) thiophene. *Macromol. Chem. Phys*. **2002**, *203*, 1238–1248.

(13) Mallakpour, S.; Dinari, M. Fabrication of Polyimide/Titania Nanocomposites Containing Benzimidazole Side Groups via Sol‑Gel Process. *Prog. Org. Coat*. **2012**, *75*, 373-378.

(14) Bruma, M.; Mercer, F.; Schulz, B.; Dietel, R.; Fitch, J.; Cassidy P. Study of the Crosslinking Process in Fluorinated Poly(Imide-Amide)s Containing Pendant Cyano Groups. *High Perform. Polym.* **1994**, *6*, 183–191.

(15) Hamciuc, E.; Bruma, M.; Schulz, B.; Kopnick, T. New Silicon-Containing Poly(imide-amide)s. *High Perform. Polym*. **2003**, *15*, 347–359.

(16) Wang, C. G.; Koyama, Y.; Uchida S.; Takata, T. Synthesis of Highly Reactive Polymer Nitrile *N*-Oxides for Effective Solvent-Free Grafting. *ACS Macro Lett.* 2014, 3, 286–290.

(17) Lin, B.; Xu, X. Preparation and Properties of Cyano-Containing Polyimide Films Based on 2,6-Bis(4-aminophenoxy)-benzonitrile. *Polym. Bull*. **2007**, *59*, 243–250.

(18) Ghosal, K.; Freeman, B. D. Gas Separation Using Polymer Membranes: An Overview. *Polym. Adv. Technol*. **1994**, *5*, 673-697.

(19) Koros WJ, Hellums MW. Gas Separation Membrane Material Selection Criteria: Differences For Weakly And Strongly Interacting Feed Components. Fluid Phase Equilibria **1989**, *53*, 339-354.

(20) Robeson, L. M. Correlation of Separation Factor versus Permeability for Polymeric Membranes. *J. Membr. Sci*. **1991**, *62*,165-185.

(21) Robeson, L. M. The Upper Bound Revisited. *J. Membr. Sci*. **2008**, *320*, 390-400.

(22) Sen, S.K. Banerjee, S. High T_g, Processable Fluorinated Polyimides Containing Benzoisoindoledione Unit and Evaluation of their Gas Transport Properties. *RSC Adv*. **2012**, *2*, 6274-6289.

(23) Ghosh, A.; Sen, S. K.; Banerjee, S.; Voit, B. Solubility Improvements in Aromatic Polyimides by Macromolecular Engineering. *RSC Adv*. **2012**, *2*, 5900-5926.

(24) Chern, Y. T.; Twu, J. T.; Chen, J. C. High Tg and High Organosolubility of Novel Polyimides Containing Twisted Structures Derived from 4-(4-Amino-2-chlorophenyl)-1-(4-aminophenoxy)-2,6-di-tert-butylbenzene. Eur. Polym. J. **2009**, *45*, 1127-1138.

(25) Mallakpour, S.; Dinari, M. High Performance Polymers in Ionic Liquid: A Review on Prospects for Green Polymer Chemistry. Part II: Polyimides and Polyesters. *Iran. Polym. J*. **2011**, *20*, 259-279.

(26) Ghosh, M. K.; Mittal K. L. (Eds.), *Polyimides: Fundamentals and Application*, Marcel Dekker, New York, 1996.

(27) Takekoshi T. (Eds.), Kirk-Othmer Encyclopedia of Chemical Technology, Wiley, New York, 19 (1996) 813–837.

(28) Tao, L. Yang, H. Liu, J. Fan, L. Yang, S. Synthesis and Characterization of Highly Optical Transparent and Low Dielectric Constant Fluorinated Polyimides. *Polymer* **2009**, *50*, 6009-6018.

(29) Jang, W.; Shin, D.; Choi, S.; Park, S.; Han, H. Effects of Internal Linkage Groups of Fluorinated Diamine on the Optical and Dielectric Properties of Polyimide Thin Films. *Polymer* **2007**, *48*, 2130-2143.

(30) Wang, C.; Chen, W.; Chen, Y.; Zhao, X.; Li, J.; Ren, Q. Synthesis and Properties of New Fluorene-based Polyimides Containing Trifluoromethyl and Isopropyl Substituents. *Mater. Chem. Phys*. *2014*, *144*, 553-559.

(31) Yang, C. P.; Hsiao, S. H.; Chen, K. H. Organosoluble and Optically Transparent Fluorine-Containing Polyimides Based on 4,4'-Bis(4-amino-2-trifluoromethylphenoxy)-3,3',5,5'-tetramethylbiphenyl. *Polymer* **2002**, *43*, 5095–5104.

(32) Kute, V.; Banerjee, S. Polyimides 7: Synthesis, Characterization, and Properties of Novel Soluble Semifluorinated poly(ether imide)s. *J. Appl. Polym. Sci*. **2007**, *103*, 3025–3044.

(33) Park, J. Y.; Paul, D. R. Correlation and Prediction of Gas Permeability in Glassy Polymer Membrane Materials via a Modified Free Volume Based Group Contribution Method. *J. Membr. Sci*. **1997**, *125*, 23-39.

(34) Moe, M. B.; Koros, W. J.; Hoehn, H. H.; Husk, G. R. Effects of Film History on Gas Transport in a Fluorinated Aromatic Polyimide. *J. Appl. Polym. Sci*. **1988**, *36*, 1833-1846.

(35) Paul, D. R. Gas Sorption and Transport in Glassy Polymers. *Ber. Bunsenges Phys. Chem*. **1979**, *83*, 294-302.

(36) Dinari, M.; Ahmadizadegan, H. Synthesis, Structural Characterization and Properties of Novel Functional Poly(ether imide)/Titania Nanocomposite Thin Films. *Polymer* **2014**, *55*, 6252-6260.

(37) Lee, W. M. Selection of Barrier Materials from Molecular Structure. *Polym. Eng. Sci*. **1980**, *20*, 65-69.

(38) Guiver, M. D. Robertson, G. P.; Dai, Y.; Bilodeau, F.; Kang, Y. S.; Lee, K. J.; Jho, J. Y.; Won, J. Structural Characterization and Gas-transport Properties of Brominated Matrimid Polyamide. *J. Polym. Sci. A: Polym. Chem*. **2002**, *40*, 4193–4204.